Materials Today: Proceedings 41 (2021) 19–29

Contents lists available at ScienceDirect

Materials Today: Proceedings

journal homepage: www.elsevier.com/locate/matpr

Doe guided chitosan based nano-ophthalmic preparation against fungal keratitis

Nazia Hassan [a], Mohd Aamir Mirza [a], Mohammed Aslam [b], Syed Mahmood [c,d,*], Zeenat Iqbal [a,*]

[a] Department of Pharmaceutics, School of Pharmaceutical Education and Research, Jamia Hamdard, New Delhi 110062, India
[b] Department of Pharmaceutics, Faculty of Pharmacy, Al Hawash Private University, Homs, Syria
[c] Department of Pharmaceutical Engineering, Faculty of Chemical and Process Engineering Technology, University Malaysia Pahang, Kuantan 26300, Pahang, Malaysia
[d] Centre for Excellence for Advanced Research in Fluid Flow (CARIFF), University Malaysia Pahang, Kuantan 26300, Pahang, Malaysia

ARTICLE INFO

Article history:
Received 24 April 2020
Received in revised form 16 June 2020
Accepted 30 September 2020
Available online 15 November 2020

Keywords:
Design of Expert
Ocular keratitis
Mucoadhesive
Antifungal
Ex-vivo
Release model

ABSTRACT

A recent upsurge in ocular infections is a pointer towards an enhanced prevalence of ophthalmic disorders, posing challenges for researchers globally. The caveats of conventional therapeutics demand a specifically designed Ocular Drug Delivery System (ODDS) and hence the primary objective of the present work is a fabrication of a *Design of Expert (DoE) guided Chitosan based Antifungal loaded Nanoparticles* (CANs), as a locoregionally effective eye formulation/drops for fungal keratitis therapy. The purported formulation was prepared using High-Pressure Homogenisation technique and was critically characterized on various parameters to check their suitability as an ODDS. The optimized formulation has fruitfully yielded irregularly spherical particles in up to a size of 200 nm and a Poly-dispersity Index (PDI) of less than 0.2 nm. The optimised formulation has further showcased a high mucoadhesion capacity thereby, suggesting the greater retention of CANs on the mucous membrane of an eye with low ocular irritancy as highlighted using HET-CAM (Hen's Egg Chorioallantoic Membrane) test. The *in-vitro* drug release study across a dialysis membrane has indicated both diffusion as swelling controlled release pattern for an optimized formulation. The *ex-vivo* corneal permeation study on goat corneal tissues using a Franz-Diffusion cell also has indicated a steady increase in the permeation of drug with time for an optimized formulation. Further, the optimised formulation was found to be non-irritant and ocular safe in *ex-vivo* transcorneal toxicity studies on goat corneal tissues. In conclusion, the designing of a proposed nanosized formulation, offers a promising step towards the management of external ocular diseases with a positive attributes of high patient compliance, controlled drug delivery, prolonged drug precorneal residence time and enhanced ocular bioavailability. The optimized CANs could be further exploited as a potential ODDS.

1. Introduction

Pharmaceutical preparations and delivery systems intended for use in any section of the human eye are classified as ophthalmic preparations/Ocular Drug Delivery Systems (ODDS). Such formulations could either be designed as liquid (eye drops/eye solutions), semi-solid (ointments) or solid, to target the various afflictions of the eye [1]. The unique natural physiology of human eye offers a great challenge towards fabrication and dispensation of an efficient ODDS system which could circumvent physiological barriers [2] and limitations like corneal drainage, rapid elimination, poor bioavailability, on-site irritations and low patient compliance [3,4]. Fungal keratitis has recently emerged as a challenging research premise for developing a standard of care ODDS [5,6]. It is an ocular infection primarily characterized by corneal inflammation i.e. anterior part covering pupil. It is mainly caused by differ-

* Corresponding authors.
E-mail addresses: syedmahmood@ump.edu.my (S. Mahmood), zeenatiqbal@jamiahamdard.ac.in (Z. Iqbal).

https://doi.org/10.1016/j.matpr.2020.09.823
2214-7853/

ent species of filamentous fungi such as *Aspergillus flavus, A. fumigatus, Fusarium* spp., *Alternaria spp*., and Candida (yeast) capable of colonizing human tissue. [4,7]. Generally, the damaged integrity of an epithelial lining marks the beginning of fungal keratitis, either due to trauma or ocular disease, making the surface highly susceptible and sensitive against the fungal antigens and toxins, that are liberated into the broken epithelial lining/surface thus, leading to high degree of inflammation, corneal damage and compromised eye functions. Fungal keratitis, if neglected, has the potential to cause ocular morbidity and vision loss [8].

Over the last few years, there has been a global expansion in incidences and frequency of fungal keratitis majorly due to high use of contact lenses and eye drops having steroidal drugs, especially in patients with immune compromised conditions such as diabetes and HIV positive cases [9,10]. United States Centres for Disease Control and Prevention reported around 154 new Fungal Keratitis cases [11] amongst which 94% are associated with contact lenses. The predominant climatic conditions for fungal keratitis are generally tropical, subtropical and agriculture-based conditions in countries such as India, China and Ghana [12,13]. *Fusarium and Aspergillus spp*. are considered as the most prevalent organisms for causing fungal keratitis in India [14,15].

Conventionally, a wide range of ophthalmic preparations are available in the market such as fungizone, liposomal preparations like Ambiosome and Natamycin, but they are marred with various limitations [16]. Fungizone shows painful instillation due to use of Nadeoxycholate as surfactant, liposomal preparation has cost limitation in developing areas, Natamycin is unavailable in various regions. Additionally, most eye preparations are likely to be easily washed off by tear fluid or due to blinking, owing to its poor mucoadhesion capactity [17].

There is an unmet need wherein it seems prudent to design and develop novel formulations such as lipid nano-capsules, nanosuspensions, vesicles etc. which could emerge as a potential ODDS, with design in components of control drug release, precorneal drug residence time and ocular bioavailability [18–24]. A newer class of azole-imidazole derivative Luliconazole (LCZ), chemically, 4-(2,4-dichlorophenyl)-1,3-dithiolan-2-ylidene-1-imidazolyl acetonitrile, was explored [25]. LCZ is primarily active against filamentous fungi, Aspergillus spp. and Candida spp [25]. A Recent study has cited LCZ as a promising candidate against susceptible and resistant *A. fumigatus* isolates as compared to other polyenes and azoles [25,26]. In addition to high antifungal activity LCZ also offers a wide range of skin safety profile making it a promising candidate for both topical as well as ophthalmic preparations [27]. The adhesion capacity of ophthalmic preparation plays a prominent role in prolonging the release, therefore, for present formulation a naturally available, biodegradable, mucoadhesive polymer viz a viz chitosan was employed [28].

Taking a step forward from the above statement, the main objective of the present proposal is to fabricate a chitosan based antifungal loaded nano-ophthalmic preparation, in the form of a locoregionally applicable eye formulation/drops, for fungal keratitis therapy. The purported formulation offers improved precorneal penetration, retention, controlled release, bioavailability, patient compliance and low on-site irritations. Also, the use of a natural polymer possesses high ocular compatibility which reduces on-site irritations thus, improving patient QoL.

2. Materials and methods

The *ex-gratia* sample of LCZ was provided by Ranbaxy Laboratories Ltd Haryana. Chitosan (low, medium and high molecular weight), mucin (Type II porcine stomach) and Poloxamer-407 were supplied from Sigma Aldrich (India). All other chemical reagents used for present study were of analytical grades.

2.1. Preparation of Chitosan-based antifungal loaded nanoparticles (CANs)

CANs were prepared by mixing a chitosan solution (chitosan in 1% v/w acetic acid solution) to a previously prepared drug (luliconazole)-poloxamer mixture dropwise through micro syringe with continuous stirring on a magnetic stirrer at 1200 rpm. Further, to ensure complete dissolution the prepared solution was kept in the refrigerator for a minimum period of 24 h. After which the formulation was passed through High-Pressure Homogeniser (HPH) at 1600 bar for 7 cycles [28,29].

2.2. Experimental design employed for optimization of CANs

Box-Behnken Design (BBD), a response surface methodology was successfully employed for the optimisation of a purported formulation based on its independent variables and dependent responses as highlighted in Table 1.

2.3. Particle size and zeta potential

The particle size distribution and zeta potential of the optimized formulation, CANs was measured using Malvern Zetasizer (Nano-ZS, UK). The measurements of each sample are done in triplicate having a scattering angle and temperature of 173° and 25 °C respectively. Prior to the measurement the test samples are appropriately diluted with ultrapure water in order to reduce particle–particle interactions. Further, the mean particle size and zeta potential were determined using disposable polystyrene cuvette and fixed-glass cell respectively [30].

2.4. Scanning electron microscopy (SEM)

The lyophilised sample of CANs was placed on the carbon tape stuck to the aluminium SEM stub, Zeiss EVO40, Carl Zeiss NTS (North America) and were further examined at a focused beam of high-energy electrons with low vacuum conditions in order to determine the surface characteristics and morphology of an optimized CANs at ambient conditions [31–32].

2.5. Transmission electron microscopy (TEM)

To examine the morphology of an optimized CANs, the technique of TEM [TECNAI G2 (200 kV) FEI, Holland] was employed. A sample of prepared CANs suspension (5–10 uL) was placed dropwise onto Formvar-coated copper grids and was allowed to dry. They were further stained with 2% w/v phosphotungstic acid and dried before examining under TEM at ambient conditions [31–32].

2.6. Mucoadhesive capacity

This test is done to evaluate the mucoadhesive capacity of CANs with mucin (0.1% w/v). To this solution, CANs were dispersed and mixed on a vortex mixer. Further, the prepared mixture was incubated at a temperature of 37 °C in an oscillating thermostatic water bath. From the mixture the appropriate samples were withdrawn at a predetermined time interval and were spectrophotometrically analysed at λ_{max} 296 nm to check turbidity of the dispersion medium and was further compared with the turbidity of a native mucin solution using Shimadzu UV–1601 ultraviolet spectrophotometer (Japan) [33–35].

2.7. In-vitro drug release

The drug release pattern of CANs was assessed by a dialysis membrane (cellulose membrane, MW cut-off 12400, Sigma) study

Table 1
BBD for optimization of CANs.

Levels	Independent variables			Transformed variables
	X_1(Surfactant concentration,% w/v)	X_2(HPH Pressure, bar)	X_3(HPH cycle)	
Low	5	500	1	−1
Medium	10	1000	4	0
High	15	1500	8	1
Dependent variables: Y_1 = Particle size (nm); Y_2 = PDI				

under sink conditions for a period of 10 h. A formulation sample of 1 mL was enveloped in a prepared dialysis bag and further incubated in a 30 mL of Phosphate Buffer Saline (PBS), pH 7.4 with Tween 80 (1%, v/v) at a temperature of 37 °C with constant stirring on a magnetic stirrer at 150 rpm. Drug releasing medium (1 mL) was removed at a predetermined time interval and are freshly replaced with an equal volume of a PBS to mimic the sink conditions. The collected samples were filtered through a membrane filter of 0.22 μm, appropriately diluted and analysed spectrophotometrically at λ_{max} 296 nm for drug content determination [31–33]. The data obtained from aforementioned study was fitted into various release kinetic models for acquiring more optimized results.

2.8. Ocular irritation test

In order to analyze the ocular tolerability of prepared CANs a modified Hen's Egg Chorioallantoic Membrane (HET-CAM) test was employed. It is a widely considered qualitative method for assessing the potential irritation capcity of chemicals. In this method the chorioallantoic membrane of hen's egg were exposed to test chemicals and the adverse changes, if any, are observed, thus, determining the potential irritancy of the test sample.

For present study, 6 fertilized eggs (freshly obtained from poultry farm), each weighing 50 to 60 g, were incubated on a shaker incubator for 3 days at a temperature of 37 ± 0.5 °C. Eggs were periodically examined, physically rotated and candled to selectively remove the defective ones. Once the redness appears, the pointed end of the egg was sterilized and broken to withdraw 3 mL of egg albumin. This opening was sealed using a 70% alcohol-sterilized parafilm and heated spatula. After this the eggs are kept in equatorial position to ensure the separated development of Chorioallantoic Membrane (CAM) from the shell. On and after the fifth day of incubation, nonviable embryos were removed every day and an opening of (2 × 2 cm) was made on eggs equator on the tenth day through which a formulation, CANs sample of (0.5 mL) was instilled directly onto the CAM surface and left in contact for 5 min. After the completion of test the CAM membrane was critically examined for any vascular damage, and the time taken for an injury to occur was recorded. A 0.9% NaCl was used as a control solution (non-irritant) [36,37].

2.9. Ex-vivo corneal permeation

For ex-vivo corneal permeation experiment goat corneas were utilised and they obtained from the local slaughter house. Using a standard eye bank technique, the dissection of corne-oscleral buttons from obtained corneas were done under maintained conditions and high degree of care to reduce the chances of tissue distortion. Immediately after corneal excision, the obtained tissue was placed in a Franz Diffusion Cell having both donor as well as receiving compartments.

For present study, the receiving compartment of a Franz diffusion contains a PBS solution of 25 mM and pH 7.4. Whereas, the donor compartment of the same contains an optimized CANs formulation (1 mL). This study was carried for a period of up to 6 h and after each h, the aliquot sample of 1 mL was withdrawn from the receiving compartment and replaced with the fresh sample. The %cumulative drug permeation across the corneal membrane was analysed spectroscopically at λ_{max} 296 nm against time [26,38,40]. The data obtained from aforementioned study was fitted into various release kinetic models for acquiring more optimized results.

2.10. Ex-vivo transcorneal toxicity

The goat corneal tissues were excised and are further subjected for a histological examination. For this study, a tissue specimen was collected and fixed in a 10% neutral-buffered formalin, fixed in a paraffin wax, partitioned at 3 μm thickness and stained with hematoxylin and eosin (H&E), and Masson's trichrome (MT) stain [38–40].

2.11. Stability

To check and determine the physical stability of the lyophilized CANs, the optimized formulation was evaluated at a temperature of 4 ± 2○C or 25 ± 2○C for a period of 90 days [40,41].

3. Results and discussion

3.1. Optimization of CANs

As obtained from BBD a total of 17 formulations (Table 2.) were prepared based on independent variables and were further evaluated for their dependent responses in order to obtain an optimized formulation.

The final equations in term of coded factors for responses R1 and R2 are given below:

R1: Particle size = +255.60 + 39.00 * A + 39.63* B −41.13* C −63.00* A*B + 70.50 * A*C −2.2 *B*C + 247.33 * A2 + 69.57 * B + 5.58 * C2

R2: PDI = +0.29 + 0.11* A + 0.037 *B −0.100*C −0.050 *A*B + 0.13*A*C −0.025*B*C + 0.40 *A + 0.054 *B2 + 0.029*C2

In aforementioned equations, the A and B positive coefficients, indicates that the Particle Size (PS) and Poly-Dispersity Index (PDI) increases with the corresponding increase in HPH cycle and pressure, while a negative coefficient of C indicates that PS and PDI decreases with the increase in concentration of poloxamer respectively. 3D response surface plots showing the influence of factors on the responses R1 and R2 are presented in Fig. 1. (A and B) respectively. In order to determine those factors that affect response the most, perturbation graphs were plotted as represented in Fig. 2. (A and B). The steep slope with factor C indicates that the PS and PDI decreased with the increase in poloxamer concentration since, increase in polymer concentration gave repelling force to other particles, thereby, preventing agglomeration or Ostwald ripening [30]. The sharp decline in PS and PDI was observed with the increase in HPH pressure till a middle value, however, with the further increase in HPH pressure, the PS increased, which can be attributed to the aggregation of particles with further increase in HPH pressure (Figs. 1 & 2).

Table 2
BBD highlighting independent variables (HPH pressure, HPH cycle and surfactant concentration) and dependent responses (particle size, and PDI).

Runs	HPH pressure	HPH cycle	Surfactant conc.	Particle size	PDI
1	1.00	0.00	−1.00	828	0.8
2	0.00	−1.00	−1.00	443	0.4
3	1.00	1.00	0.00	832	0.8
4	0.00	1.00	1.00	344	0.3
5	−1.00	11.00	0.00	762	0.7
6	0.00	0.00	0.00	256	0.2
7	1.00	0.00	1.00	990	0.9
8	**0.00**	**−1.00**	**1.00**	**216**	0.2
9	1.00	−1.00	0.00	931	0.9
10	0.00	0.00	0.00	253	0.3
11	0.00	1.00	−1.00	650	0.6
12	0.00	0.00	0.00	260	0.32
13	−1.00	0.00	−1.00	882	0.8
14	−1.00	−1.00	0.00	673	0.6
15	0.00	0.00	0.00	252	0.24
16	1.00	0.00	1.00	452	0.4
17	0.00	0.00	0.00	257	0.4

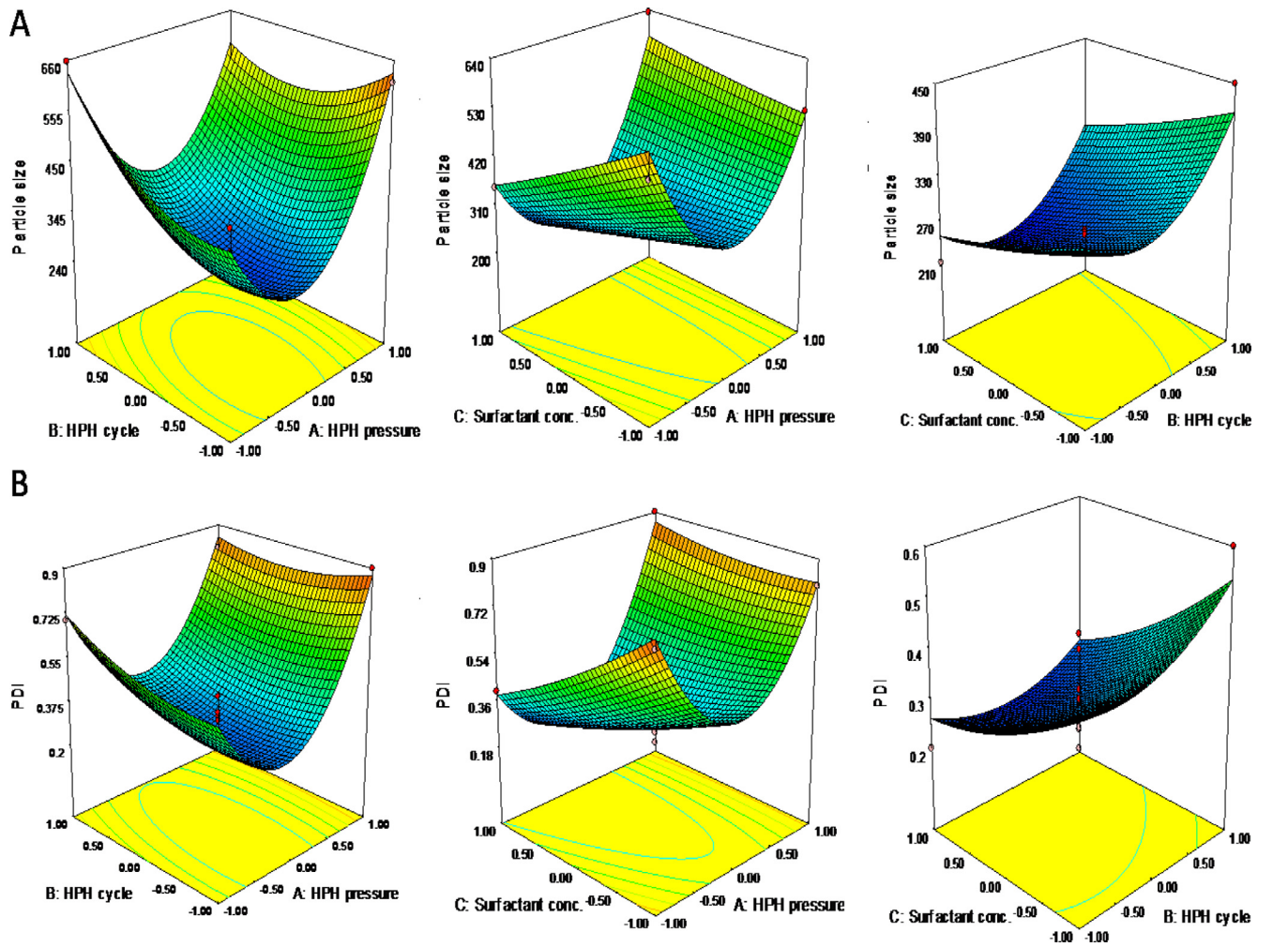

Fig. 1. 3D-Response surface graphs showcasing the effect of independent variables on dependent responses (A) particle size; (B) PDI.

Further, the formulation having a minimum PS and PDI of 216 nm and 0.2 respectively was selected as an optimized formulation (formulation coded, F8; as highlighted in Table 2.). From the obtained results, a close proximity between the values of a dependent variables and the predicted values of a BBD was observed. Further, the low values of standard deviations has confirmed the reproducibility of obtained results as highlighted in Table 3.

3.2. Particle size and zeta potential

The particle size of an optimized CANs falls in the range of 2–207 nm as presented in Fig. 3. Majority of particles (85.5%) were of the size 206.6 nm while only 14.5% were below 10 nm in size, as represented in Fig. 4. As highlighted from the obtained results, the molecular weight of chitosan has sufficiently affected the size and surface charge of an optimized formulation. With the increase in

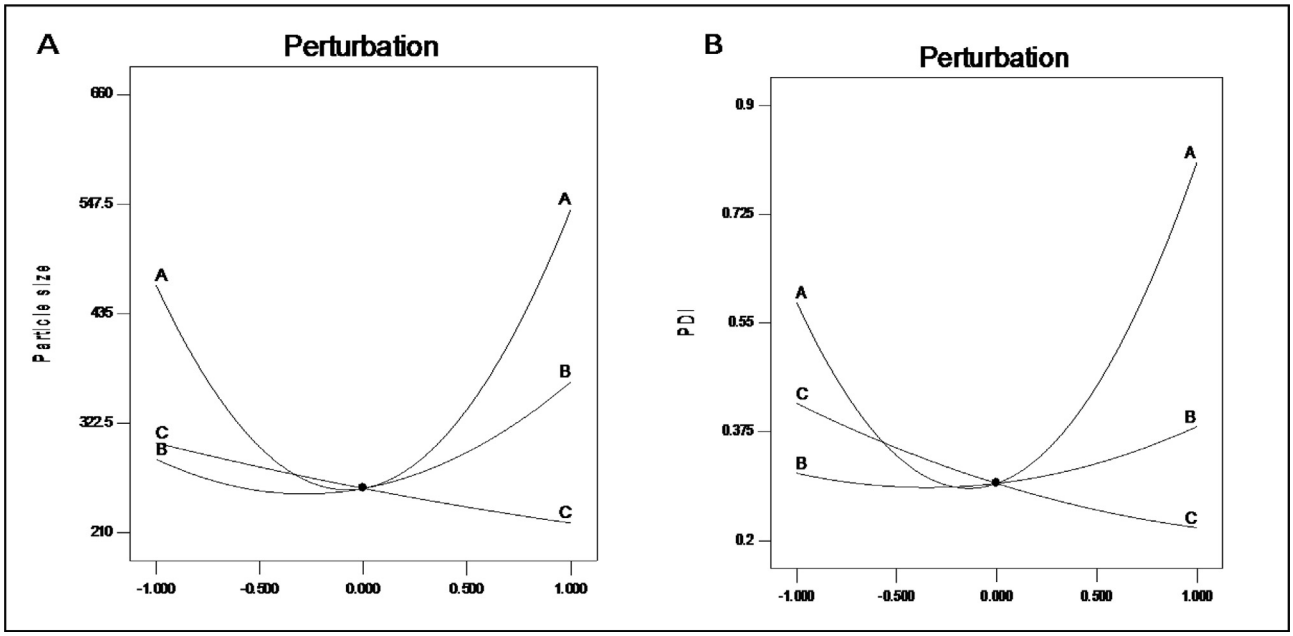

Fig. 2. Perturbation plot showcasing the effect of independent variables on dependent responses A) Particle size; B) PDI.

Table 3
Actual and predicted values from BBD.

Formulation	Composition			Response	
	HPH pressure (bar)	HPH cycle	Poloxamer conc (% w/v)	Particle size (nm)	PDI
CANs (predicted)	Coded values			214.03	0.19
	0.00	0.00	1		
CANs (actual)	Actual values			216.6 ± 0.4	0.2 ± 0.03
	1000	4	10		

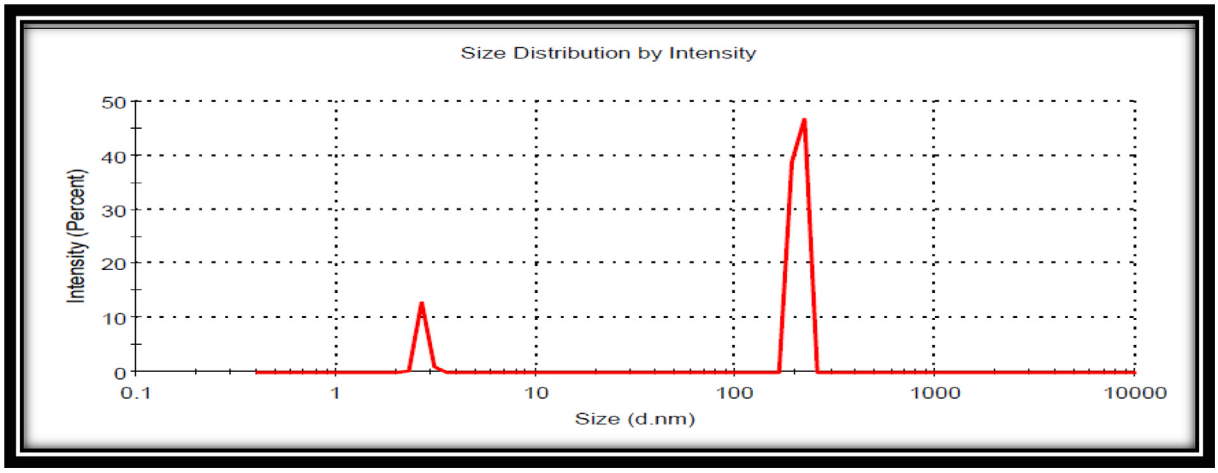

Fig. 3. Particle size of an optimized formulation (F8).

molecular weight, particle size also increases. This can be attributable to the presence of a longer molecular chains which are naturally entangled and produces a larger particle size. On contrary, the overall size distribution (PDI less than 0.2) was remained unaltered with increasing molecular weight thus, indicating the homogeneity of the prepared CANs. Further, surface charge also increases with increase in chitosan molecular weight as the negatively charged mucin of ocular surface strongly binds with a positively charged chitosan layer thus, changing zeta-potential to positive [30,32].

3.3. SEM

The surface characteristics and morphology of an optimized CANs (F8) were revealed as an irregularly shaped spherical nanoparticles with slightly smooth surface appearance as presented in Fig. 5 (B-D). The morphology of pure drug (luliconazole) was also checked for comparison [Fig. 5 (A)].

The optimized formulation (F-8) of prepared CANs has yielded irregular spherical particles with a smooth surface appearance at

Peak 1:	206.6	85.5	14.96
Peak 2:	2.719	14.5	0.1270
Peak 3:	0.000	0.0	0.000

Fig. 4. The particle size distribution of an optimized CANs (F8).

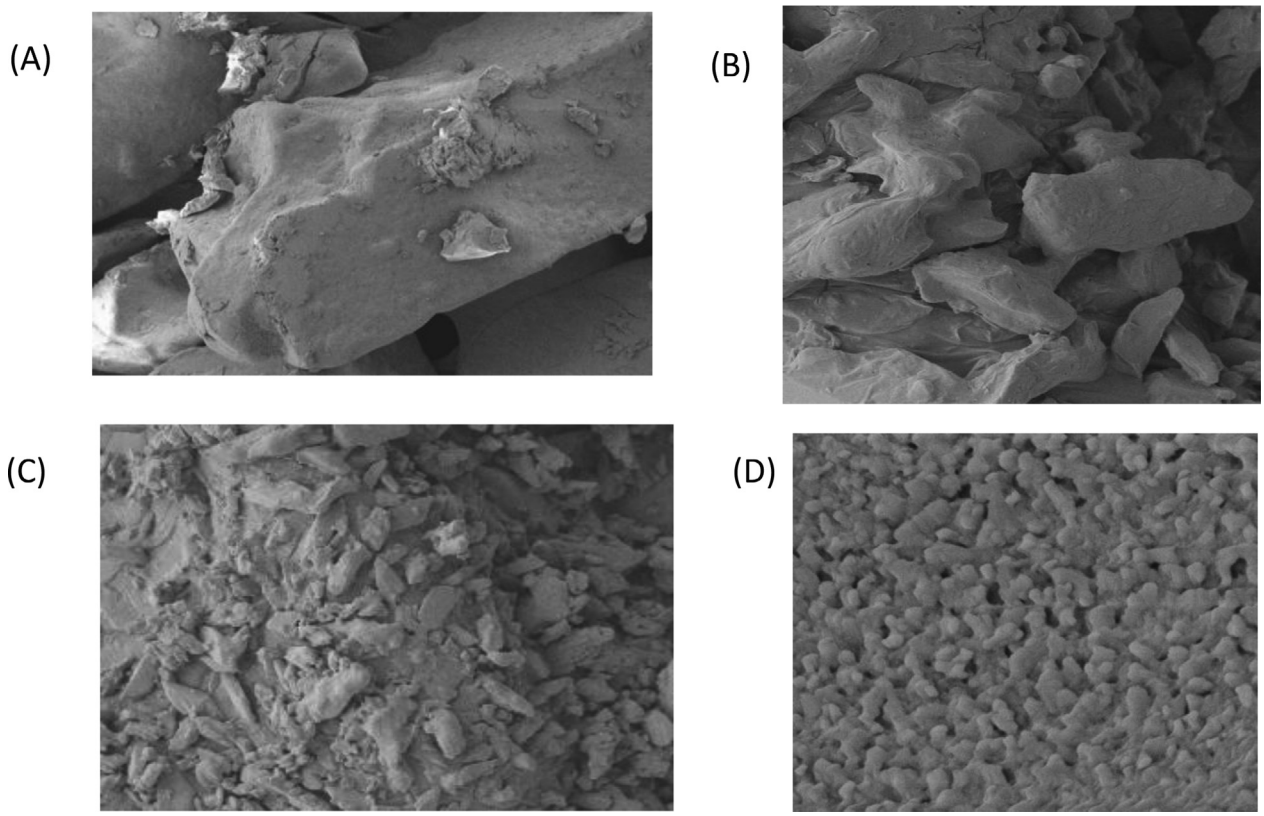

Fig. 5. SEM micrographs illustrating the surface morphology of (A) pure drug; (B) CANs after 1st cycle of HPH (1 cycle 500 bar) (C) CANs after 4th cycle of HPH (1000 bar) (D) CANs after 8th cycle hph(1000 bar).

increased HPH cycles, on the contrary, the pure drug has displayed an irregular and rough surface morphology [32].

3.4. TEM

The optimized formulation (F8) of prepared CANs revealed to have a spherical shape with a clear outline and a visible core as presented in Fig. 6 [32].

3.5. Mucoadhesive capacity

The resultant changes in the absorbance values of an optimized CANs upon incubation with 0.1% mucin dispersion are was observed. The appearance of turbidity was marked as the point for mucoadhesion. Among the three formulations, high molecular weight chitosan (hmw) nanoparticles (NPs) shows high absorbance values which indicates their high adhesion capacity with mucin, followed by medium molecular weight chitosan (mmw) NPs and low molecular weight (lmw) NPs as the increase in chitosan molecular weight results in an increase number of positively charged units which shows stronger interactions with a negatively charged mucin particles [33]. Therefore, the increased interaction of Chitosan with mucin suggest the greater retention of the CANs on the mucous membrane of an eye [33–35].

3.6. In-vitro drug release

The *in-vitro drug* release of an optimized CANs, high; medium; low formulations [each containing 1% API (w/v)] are presented in Fig. 7. The release pattern of all three formulations has shown a biphasic release rate which is as follows; first initial burst release followed by a prolonged release (Fig. 7). After 1 h, the % Cumulative Drug Release (%CDR) was found to be 26.26%, 29.0% and 55% from CANs I, II and III respectively. The

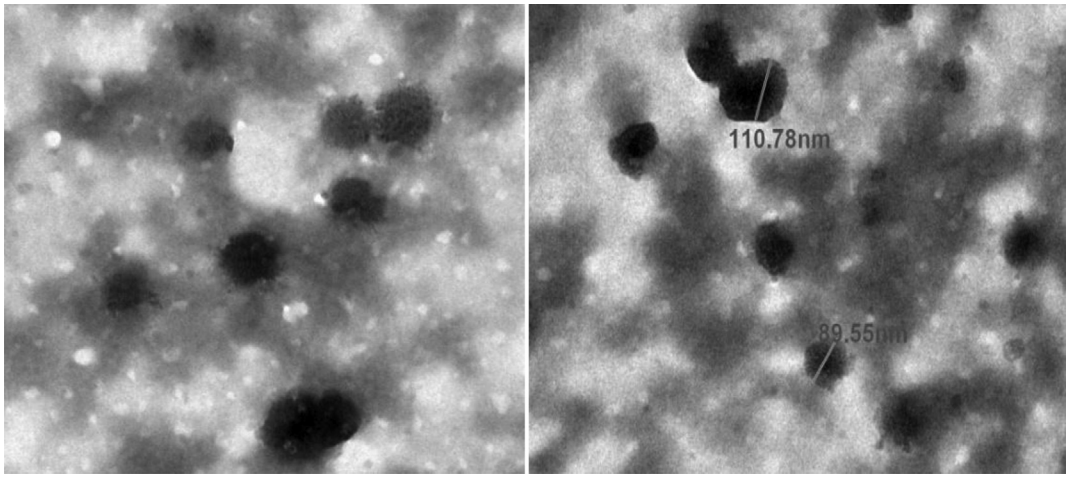

Fig. 6. TEM images of optimized CANs.

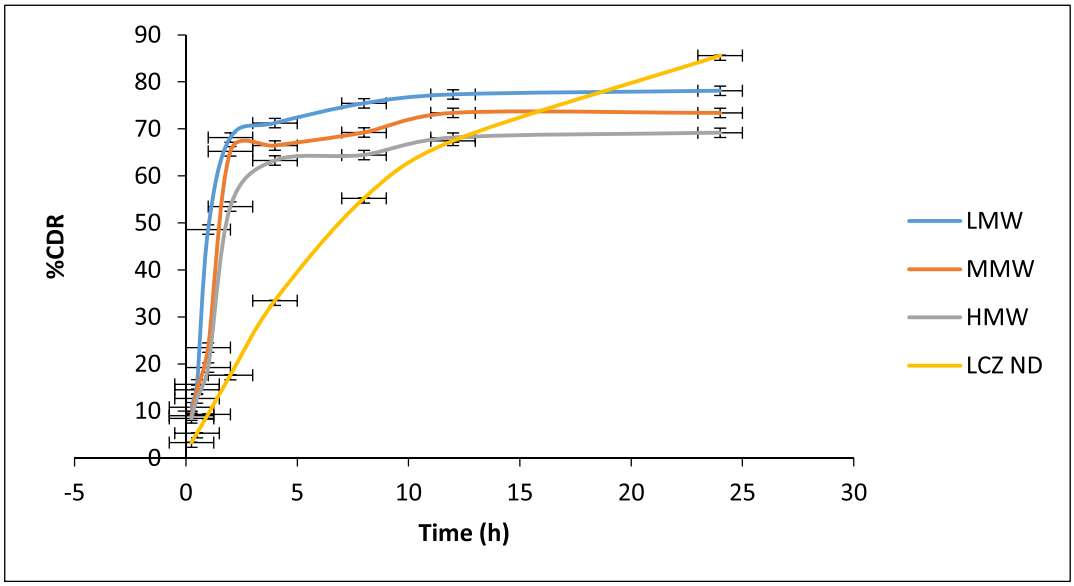

Fig. 7. In-vitro drug release profile (mean ± SD, n = 1).

initial burst release of CANs I was mainly due to the rapid desorption and diffusion of drug molecules. The highest %CDR of CANs III highlights that smaller the particle size; smaller will be the surface area in order to facilitate the drug release process [31–33]. Further, the amount of drug released from CANs I, II and III was found to be at 10 h was 83%, 86% and 88% respectively. Besides the three aforesaid preparations, a pure drug nano-dispersion (LCZ ND) was also prepared and checked simultaneously for comparison.

The aforementioned release data was incorporated into various kinetic models as shown in Table 4. As obtained from the regression coefficient the best-fit release model was found to be Korsmeyer–Peppas for the optimized formulation indicating drug release to follow both diffusions as well as swelling controlled release [33].

3.7. Ocular irritation test

The optimized CANs were found to be ocular non-irritant as well as well-tolerated (Fig. 8) for up to 8 h (mean score 0) and for 24 h (mean score 0.33) as represented in Table 5 [36,37].

3.8. Ex-vivo corneal toxicity

This test has showcased that no significant changes were observed when cornea was incubated in a PBS (Fig. 9 A). However, an irritation of superficial epithelial cells takes place, when the cornea was incubated in 0.1% w/v of sodium dodecyl sulphate solution (Fig. 9 B).

Further, the incubation of cornea with CANs has not displayed any destructive effect as presented in Figure C-E. The corneal structure and integrity were found to be unaffected visibly thus, the obtained results demonstrate ocular safety of CANs (F8) [38–40].

3.9. Ex-vivo transcorneal permeation

The *ex-vivo* %cumulative drug permeated at 6th hour across the goat corneal membrane has shown a steady increase with time (Fig. 10). The obtained permeation profile was fitted to various kinetic models and was found to best fit with zero-order kinetics, i.e. the rate of permeation was independent of the amount of drug permeated at various time points. The percentage cumulative amount of drug permeated at 6th hour from LMW, MMW, HMW

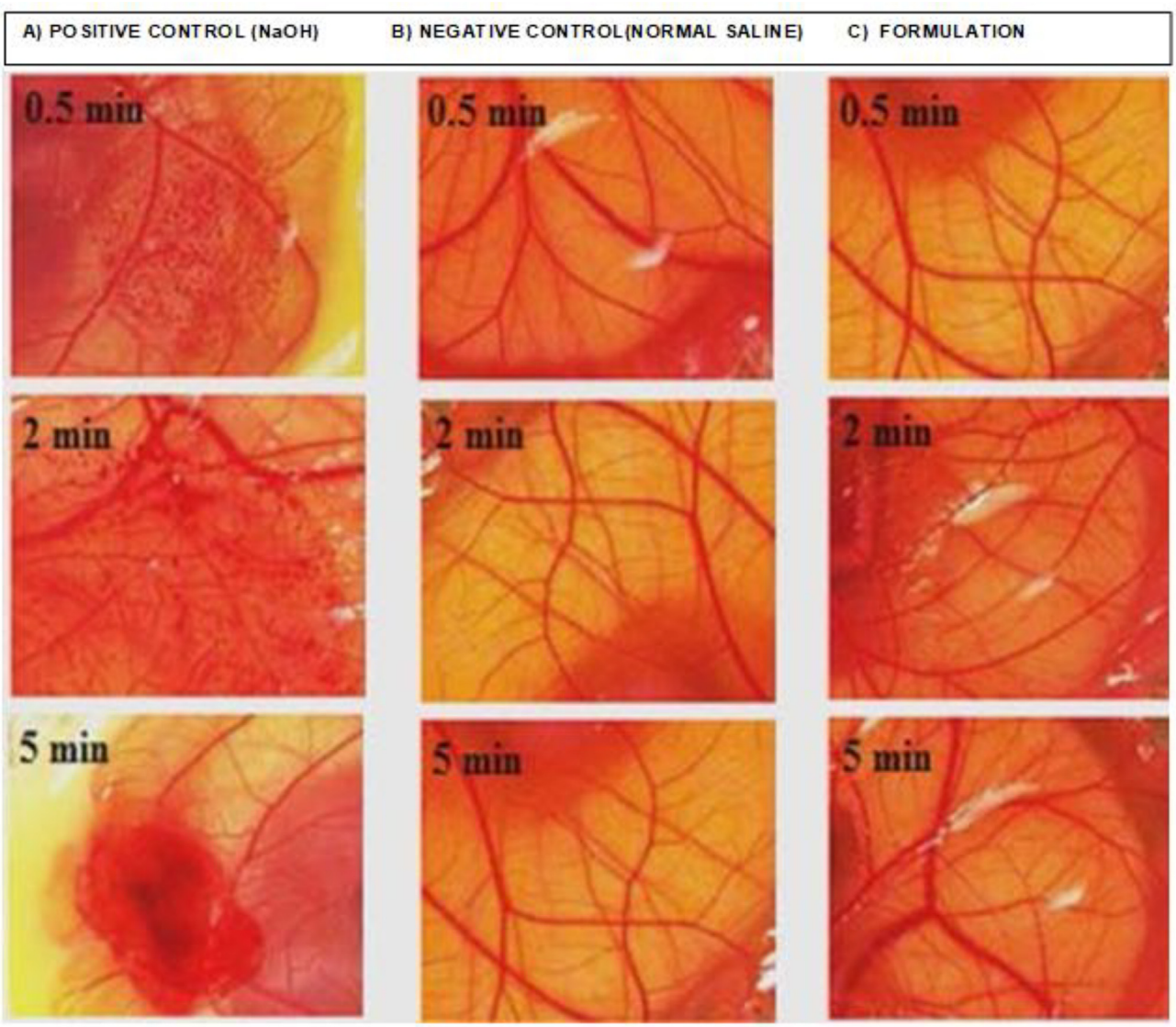

Fig. 8. Vascular responses at 0.5, 2 and 5 min post topical application of (A) 0.1 M NaOH solution, (B) saline solution, (C) CANs (F8).

Table 4
Release kinetic models.

Formulation	Zero-order model		First-order model		Higuchi model		Korsmeyer model	
	R^2	K_0	R^2	K_1	R^2	K_H	R^2	K
CANs II	0.099	25.18	0.738	1.727	0.964	0.067	**0.980**	2.479
CANs III	0.109	11.72	0.990	1.937	0.965	0.034	0.907	2.553

CANs and LCZ ND was found to be 19.26%, 17.23%, 14.61% and 60.27% respectively.

Permeation curve depicts that HMW CANs shows least penetration than LMW and MMW CANs. While the formulation without chitosan showed burst and immediate-release (LCZ ND) [38–40].

3.10. Stability

Stability studies showcases a preferable physicochemical stability pattern under study conditions with no indication of aggregation or precipitation over a period of 90 days [40,41,42].

4. Conclusion

Fungal keratitis is an ocular infection characterized by the inflammation of cornea, the anterior part of the human eye covering pupil. It is mainly caused by different species of Filamentous fungi such as Aspergillus flavus, Aspergillus fumigatus, Fusarium spp., Alternaria spp., and Yeasts such as Candida capable of colonizing human eye tissues. Despite numerous scientific efforts, efficient ocular drug delivery remains a challenge for the pharmaceutical scientists owing to the unique physiological structures of eye, rapid elimination of applied drug subsequently leading to poor bioavailability over and into the ocular tissues. Henceforth, the designing of a luliconazole loaded nanosized

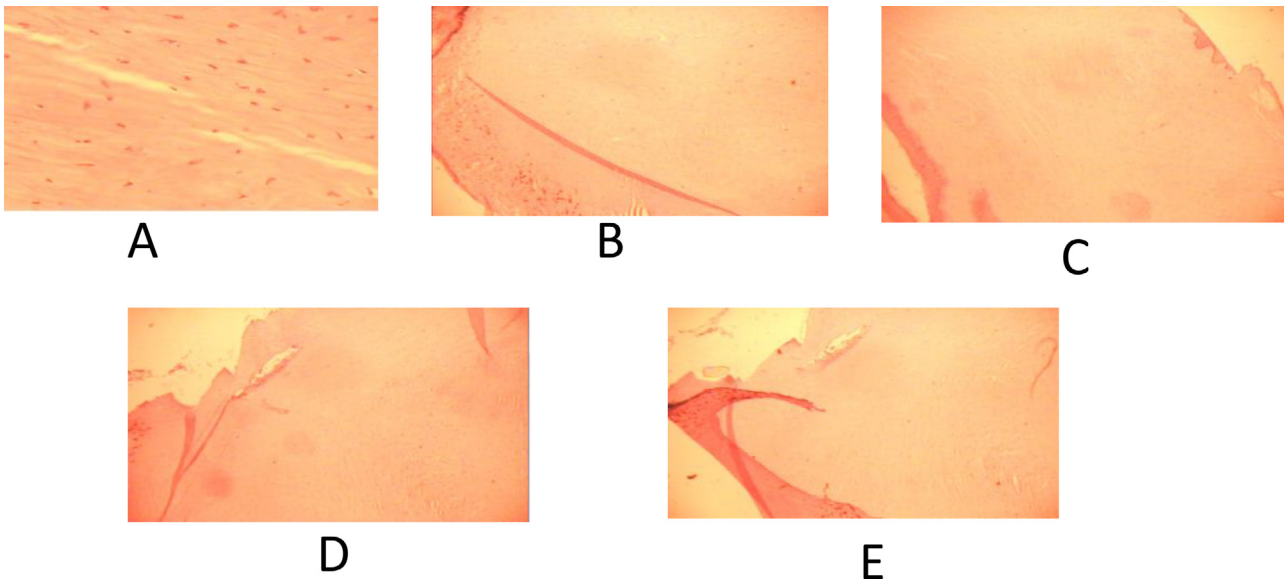

Fig. 9. Histological sections of excised goat cornea, stained with haematoxylin-eosin.

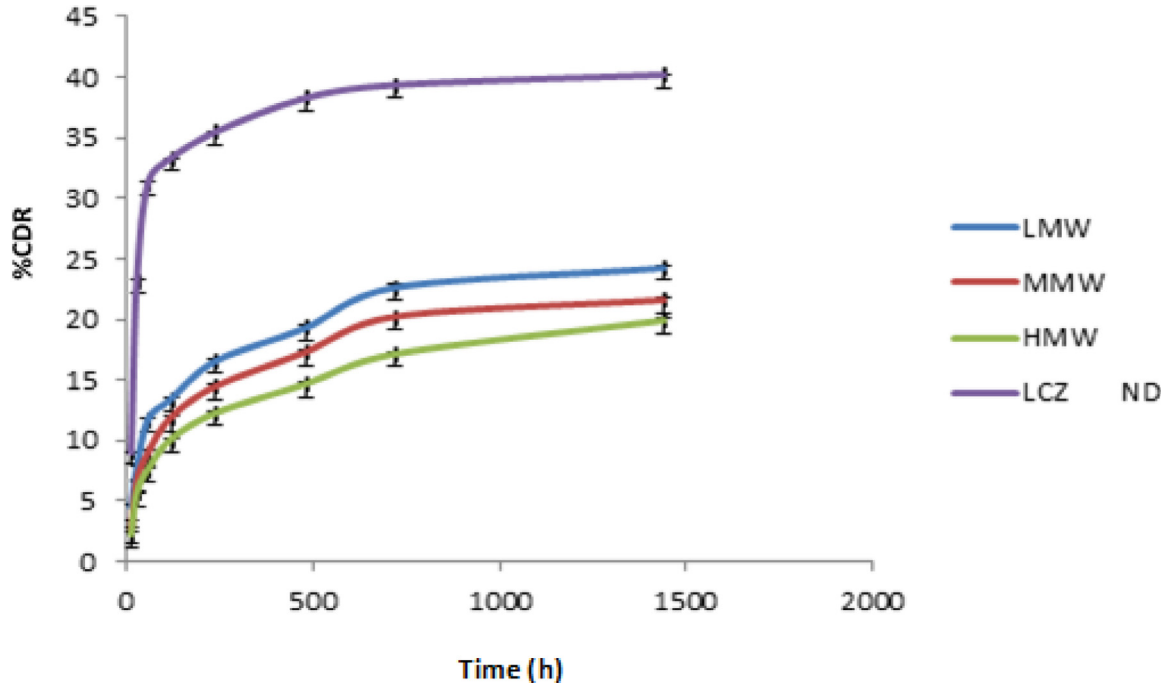

Fig. 10. Ex-vivo transcorneal permeation profile through goat cornea (mean ± SD, n = 1).

system with improved patient compliance, drug delivery, precorneal drug residence time and ocular bioavailability offers a trending platform in the field of ocular infections/diseases. Luliconazole, being a newer class of imidazole antifungal drug has not been much exploited for ocular delivery but it has shown a high activity, Minimum Inhibitory Concentration (MIC) against the major virulent pathogens of fungal keratitis in various studies, thereby making its selection for the designing of a purported formulation a novel choice. In conclusion, it is deduced that the positively charged CANs comprising chitosan elicited significant mucoretention. The precorneal retention of CANs was higher in comparison to the drug suspension (LCZ ND). Based on its in-vitro release and pharmacokinetic profile, CANs F8 was selected as an optimized formulation for controlled ocular application of LCZ. The optimized nanoformulation exhibited an increased AUC and MRT when juxtaposed with the drug suspension. Henceforth, it is proposed that the CANs could be a viable alternative for treating ocular fungal keratitis with significantly prolonged exposure and improved ocular tolerance.

CRediT authorship contribution statement

Nazia Hassan: Writing - original draft, Investigation, Methodology. **Mohd Aamir Mirza:** Writing - review & editing. **Mohammed**

Table 5
Ocular irritation (HET-CAM) test.

		SCORES							
		TIME							
FORMULATIONS	EGGS	0	5	15	30	60	120	240	480
NORMAL SALINE	EGG 1	0	0	0	0	0	0	0	0
	EGG 2	0	0	0	0	0	0	0	0
	EGG 3	0	0	0	0	0	0	0	0
	MEAN	0	0	0	0	0	0	0	0
	EGG 1	0	0	0	0	0	0	0	0
NEGATIVE CONTROL (0.1 M NaOH)	EGG 1	0	0	3	0	0	7	0	7
	EGG 2	0	5	0	0	5	0	0	4
	EGG 3	0	0	6	0	5	0	0	5
	MEAN	0	4.6	0	0	0	4.6	0	0
FORMULATION	EGG 1	0	0	0	0	0	0	0	0
	EGG 2	0	0	0	0	0	0	0	0
	EGG 3	0	0	0	0	0	0	0	0
	MEAN	0	0	0	0	0	0	0	0.66

Aslam: Writing - review & editing. **Syed Mahmood:** Writing - review & editing, Funding acquisition. **Zeenat Iqbal:** Conceptualization, Supervision.

Declaration of Competing Interest

The authors declare that they have no known competing financial interests or personal relationships that could have appeared to influence the work reported in this paper.

Acknowledgements

Authors are thankful to support provided by Jamia Hamdard central laboratory and University Malaysia Pahang as they provide financial support in the form internal research grant (RDU 180371).

References

[1] P. Verma, A. Verma, A. Namdev, S.L. Soni, Review on Basic Concept for Ophthalmic Preparations, AJPRD 1 (2015) 1–9.
[2] A. Kalkanci, S. Ozdek, Ocular Fungal Infections, Curr. Eye Res. 36 (3) (2011) 179–189, https://doi.org/10.3109/02713683.2010.533810.
[3] M. Srinivasan, Fungal keratitis:, Curr. Opin. Ophthalmol. 15 (4) (2004) 321–327, https://doi.org/10.1097/00055735-200408000-00008.
[4] P.A. Thomas, Current Perspectives on Ophthalmic Mycoses, CMR 16 (4) (2003) 730–797, https://doi.org/10.1128/CMR.16.4.730-797.2003.
[5] A. Kumar, R. Malviya, P.K. Sharma, Recent trends in ocular drug delivery: a short review, EJAS 3 (2011) 86–92.
[6] A. Sharma, J. Taniguchi, Emerging strategies for antimicrobial drug delivery to the ocular surface: Implications for infectious keratitis, OCUL SURF 15 (2017) 670–679.
[7] K. Jisha, P.K. Sreekumari, P.S. Rajesh, K.K. Jacob and B. Jayalekha. Fungal corneal ulcers: a prospective study on the causative fungus and the response to the present treatment protocol .J. Evol. Med. Dent. Sci. 5 (2016) 1833-1826.
[8] P.R. Antas, M.M. Brito, E. Peixoto, C.G. Ponte, C.M. Borba, Neglected and emerging fungal infections: review of hyalohyphomycosis by Paecilomyces lilacinus focusing in disease burden, in vitro antifungal susceptibility and management, Microb Infect 14 (2012) 1–8.
[9] F. Stapleton, N. Carnt, Contact lens-related microbial keratitis: how have epidemiology and genetics helped us with pathogenesis and prophylaxis, Eye 26 (2) (2012) 185–193, https://doi.org/10.1038/eye.2011.288.
[10] D.C. Chang, G.B. Grant, K. O'Donnell, K.A. Wannemuehler, J. Noble-Wang, C.Y. Rao, L.M. Jacobson, C.S. Crowell, R.S. Sneed, F.M.T. Lewis, J.K. Schaffzin, M.A. Kainer, C.A. Genese, E.C. Alfonso, D.B. Jones, A. Srinivasan, S.K. Fridkin, B.J. Park, F.T. Fusarium Keratitis Investigation Team, Multistate Outbreak of Fusarium Keratitis Associated With Use of a Contact Lens Solution, JAMA 296 (8) (2006) 953, https://doi.org/10.1001/jama.296.8.953.
[11] J.J. Gorscak, B.D. Ayres, N. Bhagat, K.M. Hammersmith, C.J. Rapuano, E.J. Cohen, M. Burday, N. Mirani, D. Jungkind, D.S. Chu, An Outbreak of Fusarium Keratitis Associated With Contact Lens Use in the Northeastern United States:, Cornea 26 (10) (2007) 1187–1194, https://doi.org/10.1097/ICO.0b013e318142b932.
[12] Z. Ansari, D. Miller, A. Galor, Current Thoughts in Fungal Keratitis: Diagnosis and Treatment, Curr Fungal Infect Rep 7 (3) (2013) 209–218, https://doi.org/10.1007/s12281-013-0150-1.
[13] A.K. Leck, P.A. Thomas, M. Hagan, J. Kaliamurthy, E. Ackuaku, M. John, M.J. Newman, F.S. Codjoe, J.A. Opintan, C.M. Kalavathy, V. Essuman, C.A.N. Jesudasan, G.J. Johnson, Aetiology of suppurative corneal ulcers in Ghana and south India, and epidemiology of fungal keratitis, Br. J. Ophthalmol. 86 (11) (2002) 1211–1215, https://doi.org/10.1136/bjo.86.11.1211.
[14] R. Tilak, A. Singh, O.P. Maurya, A. Chandra, V. Tilak, A.K. Gulati, Mycotic keratitis in India: a five-year retrospective stud, J Infect Dev Ctries 4 (2010) 171–174.
[15] B. Rautaraya, S. Sharma, S. Kar, S. Das, S.K. Sahu, Diagnosis and treatment outcome of mycotic keratitis at a tertiary eye care center in eastern india, BMC Ophthalmol 11 (1) (2011), https://doi.org/10.1186/1471-2415-11-39.
[16] Y.S. Chhonker, Y.D. Prasad, H. Chandasana, A. Vishvkarma, K. Mitra, P.K. Shukla, R.S. Bhatta, Amphotericin-B entrapped lecithin/chitosan nanoparticles for prolonged ocular application, Int. J. Biol. Macromol. 72 (2015) 1451–1458, https://doi.org/10.1016/j.ijbiomac.2014.10.014.
[17] N.V. Prajna, J. Mascarenhas, T. Krishnan, P.R. Reddy, L. Prajna, M. Srinivasan, C. M. Vaitilingam, K.C. Hong, S.M. Lee, S.D. McLeod, M.E. Zegans, Comparison of natamycin and voriconazole for the treatment of fungal keratitis, Arch. Ophthalmol 128 (2010) 672–678.
[18] F.S. Habib E.A. Fouad M.S. Abdel-Rhaman D. Fathalla Liposomes as an ocular delivery system of fluconazole: in-vitro studies 88 8 2010 901 904 10.1111/j.1755-3768.2009.01584.x
[19] P. Pawar, H. Kashyap, S. Malhotra, R. Sindhu, Hp–CD-Voriconazole In Situ Gelling System for Ocular Drug Delivery: In Vitro , Stability, and Antifungal Activities Assessment, Biomed Res. Int. 2013 (2013) 1–9, https://doi.org/10.1155/2013/341218.
[20] S. Das, P.K. Suresh, R. Desmukh, Design of Eudragit RL 100 nanoparticles by nanoprecipitation method for ocular drug delivery, Nanomed. Nanotechnol. Biol. Med. 6 (2) (2010) 318–323, https://doi.org/10.1016/j.nano.2009.09.002.
[21] N.M. Davies, Biopharmaceutical considerations in topical ocular drug delivery, Clin. Exp. Pharmacol. Physiol 27 (2000) 558–562.
[22] D. Meisner, M. Mezei, Liposome ocular delivery systems, Adv. Drug Deliv. Rev 16 (1995) 75–93.
[23] P. Gershkovich, K.M. Wasan, C.A. Barta, A review of the application of lipid-based systems in systemic, dermal/transdermal, and ocular drug delivery, Crit Rev Ther Drug Carrier Syst 25 (2008) 545–585.
[24] J.J. Kang-Mieler, C.R. Osswald, W.F. Mieler, Advances in ocular drug delivery: emphasis on the posterior segment, Expert Opin Drug Deliv 11 (2014) 1647–1660.
[25] D. Todokoro, T. Suzuki, T. Tamura, K. Makimura, H. Yamaguchi, K. Inagaki, H. Akiyama, Efficacy of Luliconazole Against Broad-Range Filamentous Fungi Including Fusarium solani Species Complex Causing Fungal Keratitis, Cornea 38 (2019) 238–242.
[26] M. Abastabar, N. Rahimi, J.F. Meis, N. Aslani, S. Khodavaisy, Nabili, A Rezaei-Matehkolaei, K Makimura, H Badali; Potent activities of novel imidazoles lanoconazole and luliconazole against a collection of azole-resistant and-susceptible Aspergillus fumigatus strains, Antimicrob Agents Chemother. 60 (2016) 6916–6919.
[27] N. Hassan, M. Singh, S. Sulaiman, P. Jain, K. Sharma, S. Nandy, M. Dudeja, A. Ali, Z. Iqbal, Molecular Docking-Guided Ungual Drug-Delivery Design for Amelioration of Onychomycosis, ACS Omega 4 (2019) 9583–9592.
[28] A.A. Mahmoud, G.S. El-Feky, R. Kamel, G.E. Awad, Chitosan/sulfobutylether-β-cyclodextrin nanoparticles as a potential approach for ocular drug delivery, Int. J. Pharm 413 (2011) 229–236.
[29] I.P. Kaur, C Rana, H Singh; Development of effective ocular preparations of antifungal agents, JOPT 24 (2008) 481–494.
[30] R.D. Schoenwald, P. Stewart, Effect of particle size on ophthalmic bioavailability of dexamethasone suspensions in rabbits, J. Pharm Sci. 69 (1980) 391–394.
[31] M.K. Pathak, G. Chhabra, K. Pathak, Design and development of a novel pH triggered nanoemulsified in-situ ophthalmic gel of fluconazole: ex-vivo

transcorneal permeation, corneal toxicity and irritation testing, DRUG DEV IND PHARM 39 (2013) 780–790.
[32] B. Mandal, K.K. Halder, S.K. Dey, M. Bhoumik, M.C. Debnath, L.K. Ghosh, Development and physical characterization of chloramphenicol loaded biodegradable nanoparticles for prolonged release, Pharmazie 64 (2009) 445–449.
[33] N.M. Davies, S.J. Farr, J. Hadgraft, I.W. Kellaway, Evaluation of mucoadhesive polymers in ocular drug delivery: I. Viscous solution, Pharm. Res 8 (1991) 1039–1043.
[34] A.M. Durrani, N.M. Davies, M. Thomas, I.W. Kellaway, Pilocarpine bioavailability from a mucoadhesive liposomal ophthalmic drug delivery system, Int. J. Pharm 88 (1992) 409–415.
[35] M.M. Mehanna, H.A. Elmaradny, M.W. Samaha, Mucoadhesive liposomes as ocular delivery system: physical, microbiological, and in vivo assessment, Drug Dev Ind Pharm 36 (2010) 108–118.
[36] H. Abdelkader, S. Ismail, A. Hussein, Z. Wu, R. Al-Kassas, R.G. Alany, Conjunctival and corneal tolerability assessment of ocular naltrexone niosomes and their ingredients on the hen's egg chorioallantoic membrane and excised bovine cornea models, Int. J. Pharm 432 (2012) 1–10.
[37] B. McKenzie, G. Kay, K.H. Matthews, R.M. Knott, D. Cairns, The hen's egg chorioallantoic membrane (HET-CAM) test to predict the ophthalmic irritation potential of a cysteamine-containing gel: quantification using Photoshop® and ImageJ, Int. J. Pharm 490 (2015) 1–8.
[38] R.G. Alany, T. Rades, J. Nicoll, J.G. Tucker, N.M. Davies, W/O microemulsions for ocular delivery: Evaluation of ocular irritation and precorneal retention, J Control Release 111 (2006) 145–152.
[39] G. Buech, E. Bertelmann, U. Pleyer, I. Siebenbrodt, H.H. Borchert, Formulation of sirolimus eye drops and corneal permeation studies, J Ocul Pharmacol Ther 23 (2007) 292–303.
[40] Mahmood, S., Taher, M., Mandal, U.K., Experimental design and optimization of raloxifene hydrochloride loaded nanotransfersomes for transdermal application. Int. J. Nanomedicine, 9 (2014) 4331-4346.
[41] A. Salgueiro, M.A. Egea, M. Espina, O. Valls, M.L. García, Stability and ocular tolerance of cyclophosphamide-loaded nanospheres, J Microencapsul 21 (2004) 213–223.
[42] S. Mahmood, U.K. Mandal, B. Chatterjee, Transdermal delivery of raloxifene HCl via ethosomal system: Formulation, advanced characterizations and pharmacokinetic evaluation, Int J Pharmaceut. 542 (2018) 36–46.